"Science Stays True Here"
Biological and Chemical Research, Volume 2014, 26-33 | Science Signpost Publishing

Numerical Analysis of Blood Flow in the Dysplastic Circle of Willis Using One-dimensional Patient-Specific Model

Xunjie YU[1], Changjin JI[1], Ying HE[2]*, and Junyuan CHEN[1]

1. Department of Modern Mechanics, University of Science and Technology of China,Hefei, 230027, China

2. School of Energy and Power Engineering, Dalian University of Technology

Received: September 25, 2014 / Accepted: October 19, 2014 / Published: November 25, 2014

Abstract: In this work, aiming at studying the impact of anatomical variations in the circle of Willis on the capacity of collateral blood supply, a computational scheme for constructing the patient-specific one-dimensional geometric models has been developed based on computerized tomography images. The lengths and diameters for different structures of circle of Willis (CoW) are extracted. Blood flow in the circle of Willis is modeled by using one dimensional equations derived from axisymmetric Navier-Stokes equations for flow in elastic and compliant vessels.Two frequently observed anatomical variations of the CoW (ACA, A1 aplasia and ACA, A1 hypoplasia) have been simulated. The results are compared with those of the complete and well-balanced CoW. The results show that, in the complete and well balanced CoW, it is almost not required to use collateral pathways through the anterior communicating artery (ACoA) to regulate the blood supply in the brain. However, in the unilateral A1 aplasia (non-visualization of one A1) and A1 hypoplasia (less than 90% in size of dominant A1) structure, the role of ACoA becomes considerably important. Moreover, the result of our patient-specific models show that the ACoA outward hypertrophic remodeling can compensate the blood flow in the contralateral side well, which is different from that obtained by the previous average anatomical geometric models.

Keywords: The circle of Willis, Patient-specific modeling, Anatomical variation, Outward hypertrophic remodeling, 1D modeling.

1. Introduction

Stroke is a rapid loss of brain function due to disturbance in the blood supply to the brain and can cause permanent neurological damage and death. Transient ischemic attack (TIA) and blockage caused by the rupture of aneurysm are the common risk factors for stroke. As the primary collateral pathways in the brain, the circle of Willis plays a critical role in maintaining the sufficient blood supply to the brain tissue. Its ring-like structure will reroute the flow from the contralateral side to compensate the ischemia region. Unfortunately, it is reported that about 50% of the population has a circle of Willis with at least one artery absent or hypoplastic. The incompleteness of structure will increase the risk of stroke in patients with severe stenosis. Therefore, the study of blood flow in the circle of Willis with a specific structure is extremely necessary and can help us understand deeply the compensatory capacity of the circle of Willis.

For the past decades, extensive modeling work of hemodynamics in CoW has been conducted. Ferrandez et al carried out 2D simulation of blood flow in CoW with integration of a new active boundary condition to study the influence of blood autoregulation. They concluded that a missing or dysfunction of right A1 segment of anterior cerebral artery is the worst case from the view of outflow balance. Long et al. performed 3D numerical studies of blood flow for

Corresponding author:

Ying HE, School of Energy and Power Engineering, Dalian University of Technology. Email: heying@dlut.edu.cn.

exploring the relationship between different CoW configurations and stenosis severities of CCA. It is revealed that when the stenosis is not greater than 86%, the additional pathways are able to raise the ipsilateral MCA pressure considerably without reducing the flow perfusion.

Recently, Jou et al demonstrated that cross-flow exists at every ACoA through investigation of different configurations of CoW with aneurysms. It is shown that after formation of the ACoA aneurysm, mean cross-flow appears to decrease by 22% with patent PcoAs and by 37% with occluded PCoAs. A larger and shorter ACoA allows flow through ACoA easily and leads to higher hemodynamics forces on the artery. The studied anatomical data show that the patients with cerebral aneurysms have larger ACoAs, implying that there exists some interactions between the geometry of ACoA and cerebral aneurysms.

In Xu's work, a numerical study on the influence of A1 dysplasia or hypoplasia on anterior communicating artery aneurysms was explored. The diameter of A1 on one side was fixed while the diameter of A1 on other side was decreased and eliminated. It is found that when the diameter of the non-dominant A1 gradually decreases, wall shear stress (WSS) and flow velocity increases in the dominant bifurcation. When the aneurysm is formed and grows, WSS and flow velocity gradually decreases, which suggests that A1 dysplasia/hypoplasia is potential risk in the formation of ACoA.

1D modeling is an effective method to study the effects of anatomical variations and occlusions on cerebral blood flows. In the work of Liang et al., nine topological structures were employed to investigate the mechanism of cerebral hyperperfusion following carotid artery surgery. It is pointed out, in a certain CoW structure, the diameters of the cerebral communicating arteries and the severity of carotid artery stenosis both contribute to the post-CAS hyperperfusion rates. Alastruey et al. gave the same conclusion as that of Ferrandez et al that the worst scenario in terms of reduction in the mean cerebral outflows is the CoW without the first segment of an anterior cerebral artery combined with an occlusion of the contralateral ICA.

Although in the above researches, the influences of anatomical variations on collateral capacities of CoW and ACoA aneurysms have been extensively explored. To date, 1D modeling for CoW is mostly based on average anatomical data. Aiming at confirming the conclusion that a missing or dysfunctional A1 segment of ACA can lead to long-term blood flow reduction through efferent vessel, 1D numerical modeling using patient-specific structures of the CoW was conducted.

2. Methods

Governing equations

Numerous papers discuss one-dimensional model for blood flow and pressure. We employed equations derived by Olufsen. Predictingblood flow in a compliant vessel requires threegoverning equations: twoto ensure the conservation of mass and momentum,one to obey the law of elasticity. The continuity andmomentum equations may be respectively defined as:

$$\frac{\partial A}{\partial t} + \frac{\partial q}{\partial x} = 0 \tag{1}$$

$$\frac{\partial q}{\partial t} + \frac{\partial}{\partial x}\left(\frac{q^2}{A}\right) + \frac{A}{\rho}\frac{\partial P}{\partial x} = -\frac{2\pi v r}{\delta}\frac{q}{A} \tag{2}$$

The state equation in the arteries is written as

$$P(x,t) - P_0 = \frac{4}{3}\frac{Eh}{r_0}\left(1 - \sqrt{\frac{A_0}{A}}\right) \tag{3}$$

Three types of boundary conditions including inflow, outflow and bifurcation condition were established. The flow rate of the upper ascending aorta was applied as the inflow condition. At the bifurcations, the boundary conditions were represented by the conservation of mass flux and total pressure. The outflow condition is determined by Windkessel model (Fig. 1(a)), which is given by

$$\frac{\partial P}{\partial t} = R_1 \frac{\partial q}{\partial t} - \frac{p}{R_2 C_T} + \frac{q(R_1 + R_2)}{R_2 C_T} \tag{4}$$

where the total resistance $R_T = R_1 + R_2$ and the total compliance C_T of vascular bed are obtained from Olufsen's structured tree model (Fig.1(b)) of smaller arteries.

For specific α and β, the geometry of the structured tree (Fig. 1(b)) is determined by the radii of root artery. The input impedance of each segment in the structured tree is expressed as

$$Z(0,\omega) = \frac{ig^{-1}\sin(\omega L/c) + Z(L,\omega)\cos(\omega L/c)}{\cos(\omega L/c) + igZ(L,\omega)\sin(\omega L/c)} \tag{5}$$

The input impedance at bifurcation is determined by

$$\frac{1}{Z_p} = \frac{1}{Z_{d_1}} + \frac{1}{Z_{d_2}} \tag{6}$$

By setting the terminal resistance of the structured trees to be zero, we can obtained the root impedance of the structured tree, $Z1(0, \omega)$.

The frequency-dependent impedance of the Windkessel model is given by

$$Z(0,\omega) = \frac{R_T + i\omega C_T R_1 R_2}{1 + i\omega C_T R_2} \tag{7}$$

Here, The total resistance R_T for the truncated artery is assumed to be the root impedance $Z1(0,0)$ of the structured smaller arterial tree and R_1/R_T is assumed to be euqal to 0.2. On the other hand, the compliance of every arterial segment is defined as

$$C = \frac{dA}{dp} \approx \frac{3A_0 r}{2Eh} \tag{8}$$

The total compliance of the smaller arterial tree is thus given by the sum of the compliances of the smaller arterial segments.

Patient-specific geometrical data of the CoW

Three sets of patient-specific data have been obtained at the 1st affliated hospital of Anhui Medical Univeristy. The 3D geometry of CoW has been reconstructed from high-resolution CT images using Simpleware software package as shown in Fig.2. The daimeters of vessel segments were measured directly in the 3D models by Simpleware. In order to get the lengths of vessels for 1D model, a scheme was developed to acquire the skeleton of CoW.

In order to get the lengths of vessels for 1D model, a scheme was developed to acquire the skeleton of CoW.The vessel regions in every slice were firstly extracted by threshold segmentation method . Subsequently, thinning filter of Simpleware was applied to the images interatively to get the barycenters of vessel regions. Since there are different braching directions for CoW, some barycenters of vessel regions may not represent those of vessel cross sections, especially in the vicinities of braching areas. The barycenters in these regions were re-searched manually as shown in the circle of Fig. 3a. After the barycenters of vessel cross sections along the flow directions were obtained (Fig. 3b), the

adjacent points for every barycenter were identified by scanning the 3×3×3 cubic region. The skeleton of CoW was thus obtained by connnecting the adjacent points (Fig. 3c). The length measurements can be acquired along the centerline of every segment. In the 1D model, 33 arterial segments were taken into consideration (Fig. 4), where the data for the arterial network of CoW were from the image measurements.

3. Results

Fig. 5 shows the blood flow waveforms in different vessels of complete CoW. It is seen that the flow rates from the left and right efferent arteries have not significant differences (Fig. 5a) and there is almost no flow passing through ACoA(Fig. 5b). These results show a favroable agreemnt with those by Alastruey et al., implying that it is almost not necessary using ACoA for the collateral regulation in the complete CoW.

The flow waveforms of left and right MCAs, PCAs, and ACAs are plotted in Fig. 6 when the left ACA, A1 is absent. It is noteworthy that despite of the existance of A1 aplasia, the flow rates of left and right ACA remain almost the same. We found that the radii of ACoA in the three structures of Fig. 2 are varied significantly, which are 0.81, 0.74, and 1.09 mm for the complete CoW, A1 hypoplasia, and A1 aplasia respectively.

For comparison, The flow rates in the CoW with A1 aplasia were simulated when the radius of ACoA was changed from 0 to 1 mm. Fig. 7a illustrates the variation of the mean flow rate in ACoA with the change of its diameter. It is flound that when the radius is less than 0.3 mm or larger than 0.8 mm, the increasing of flow rate with radius is slow, but when the radius of ACoA is larger than 0.3 mm, the mean flow rate increases considerably. Fig. 7b and Fig. 7c give the flow rate of left and right ACA when the diameter of ACoA equals to 0.4 and 0.8 mm respectively. It can be seen that there is slight reduction of flow rate in R. ACA when the radius of ACoA is 0.4 mm. If the radius of ACoA becomes 0.8 mm, the flow rates in the two sides have become almost the same. In the patient-specific model with A1 aplasia, the calibre of ACoA has been enlarged more than 0.8 mm to adequately compensate the reduction of flow in R. ACA. Hence, it is implied that even in the structure with A1 aplasia, the collateral capacity can be enhanced through the remodeling of ACoA., which can not be seen in the study by using the average anatomical data.

4. Concluding Remarks

In this work, a computational scheme for constructing the patient-specific geometric models has been developed based on CT images and one-dimensional numerical analysis has been carried out. The simulated results for the complete CoW show favorable agreement with previous 1D models, however, the resultsfor the CoW with A1 aplasia show that the ACoA outward hypertrophic remodeling can compensate the blood flow in the contralateral side well, which is different from that obtained by the previous average anatomical geometric models.

Currently, the thinning process is not totally automatic, it may be improved by using a robust approach for decomposing the biomedical geometries into tips, segments, and junctions, such as that proposed by Jiao et al. The patient-specific 1D modeling provided some insight into the influence of anatomical variations on blood flows.

Acknowledgement

This work was partially supported by the Fundamental Research Fund for the Central Universities in Dalian University of Technology (No. 852023)

References

[1] Alastruey, J, Parker, KH, Peiro J, Byrd, SM, Sherwin, SJ, Modeling of the circle of Willis to assess the effects of anatomical variations and occlusions on cerebral flows. J. Bomech., 2007, vol. 40, pp.1794-1805.

[2] Ferrandez, A, David, T.， Brown，MD , Numerical Models of Auto-regulation and blood flow in the cerebral circulation Comp. Meth. Biomech. Biomed. Eng. , 2002, Vol. 5, pp. 7-20.

[3] Jiao XM, Einstein DR, Dyedov, V, Carson JP, Automatic identification and truncation of boundary outlets in complex imaging-derived biomedical geometries, Med. Biol. Eng. Comp., 2009, Vol. 47,pp.989-999.

[4] Jou, LD, Lee, DH, Mawad, MZ, Cross-flow at the anterior communicating artery and implication in cerebral aneurysm formation, J. Biomech., 2010, Vol. 43, 2189-2195.

[5] Liang, FY, Fukasaku, K, Liu H., and Takagi S., A computational model study of the influence of the anatomy of the circle of Willis on cerebral hyperperfusion following carotid artery surgery . BioMed. Eng. Online, 2011, 10:84.

[6] Long, Q., Luppi, L., Konig CS, Rinaldo,V., Das, SK, Study of the collateral capacity of the circle of Willis of patients with severe carotid artery stenosisby 3D computational modeling, J. Biomech., 2008, Vol. 41, pp.2735-2742.

[7] Olufsen, M, Structured tree outflow condition for blood flow in larger systemic arteries, Am. J. Physiol. Heart Circ. Physiol., 276, 257-268, 1999.

[8] Xu, LY, Zhang Z., Wang H, Yu YQ, Contribution of the hemodynamics of A1 dysplasia or hypoplasia to anterior commnucating artery aneurysms: a three-dimensional numerical study, J. Comput. Ass. Tomo., 2012, Vol. 36, No. 4, pp. 421-426.

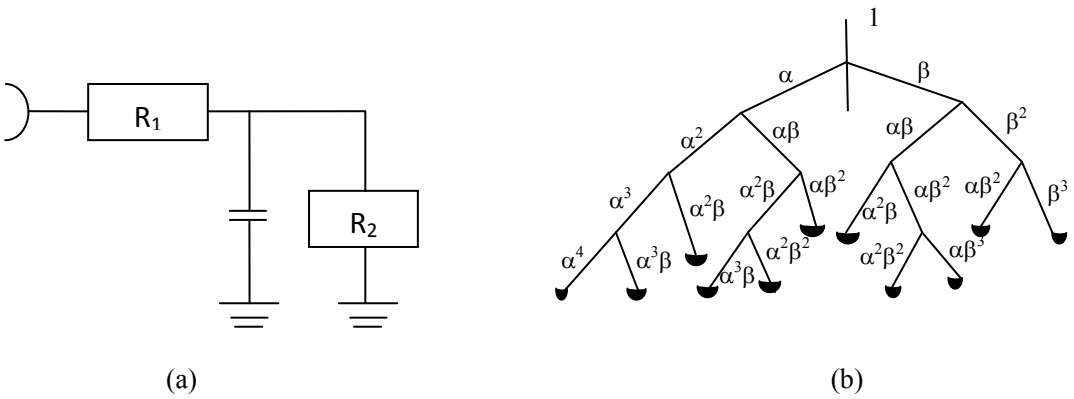

Fig. 1 The schematic diagram of the Windkessel model (a) and the structured tree model (b). At each bifurcation the radii of the daughter vessels are scaled by factors α and β

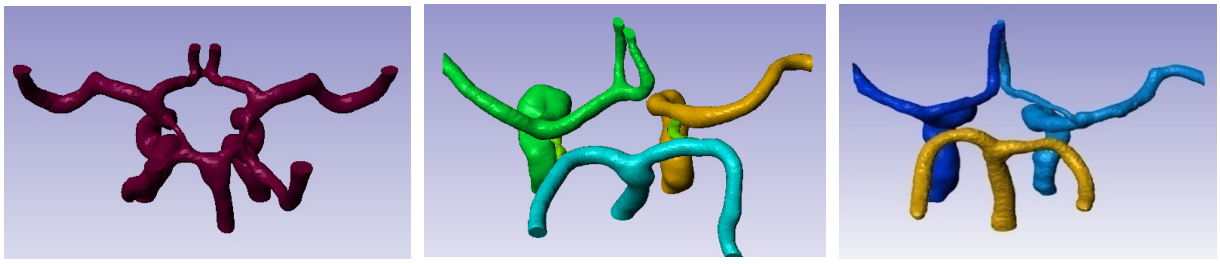

Fig. 2 3D models of CoW reconstruced from cerebral CT data (a. normal b. A1 aplasia,c. A1 hypoplasia)

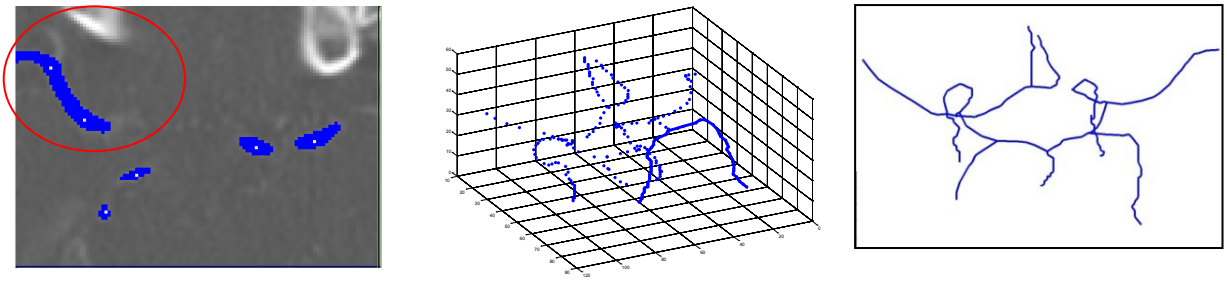

(a) (b) (c)

Fig. 3(a). Barycenters in the vessel regions of one slicing image; (b). Coordinates of the barycenters extracted from the image data; (c). Skeleton of the patient-specific CoW by connecting the adjacent points in Fig.3(b)

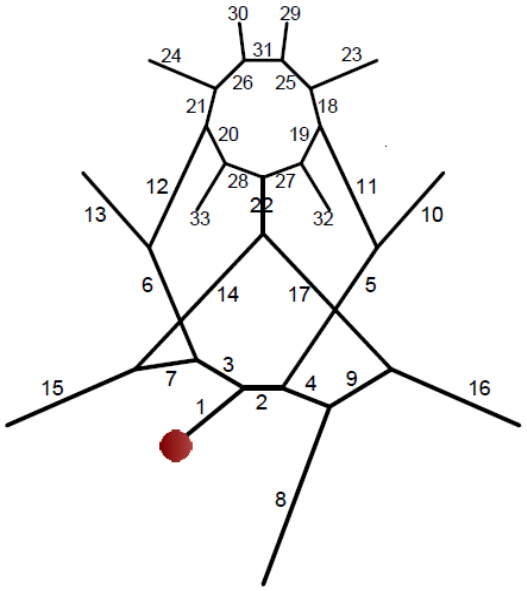

Fig. 4 1D Model of the SimulatedArterial Network

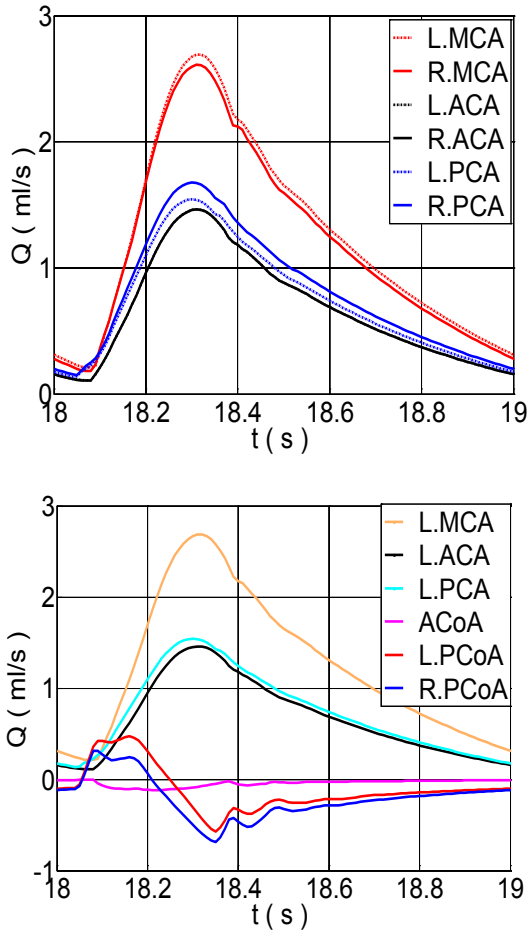

Fig. 5 Simulated flow waveforms in efferent arteries and communicating arteries for the complete CoW

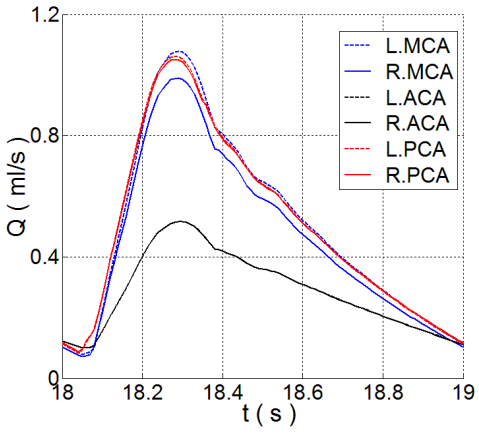

Fig. 6 Simulated flow waveforms in efferent arteries for the CoW with A1 aplasia

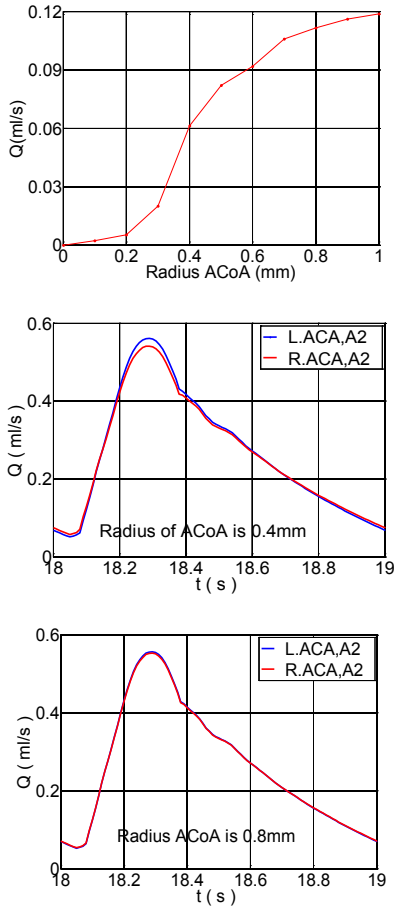

Fig. 7 (a) Mean flow rate in ACoA for different ACoA radius. (b) and (c) Flow waveforms in ACA, A2 segment while the radius of ACoA is 0.4 mm (b) and 0.8 mm (c)